Universiteit
Leiden
The Netherlands

Diversity of glucocorticoid receptor signaling: molecular mechanisms and therapeutic implications

Viho, E.M.G.

Citation

Viho, E. M. G. (2023, September 7). *Diversity of glucocorticoid receptor signaling: molecular mechanisms and therapeutic implications*. Retrieved from https://hdl.handle.net/1887/3638839

Version:	Publisher's Version
License:	Licence agreement concerning inclusion of doctoral thesis in the Institutional Repository of the University of Leiden
Downloaded from:	https://hdl.handle.net/1887/3638839

Note: To cite this publication please use the final published version (if applicable).

2

The development of novel glucocorticoid receptor antagonists: From rational chemical design to therapeutic efficacy in metabolic disease models

JAN KROON*, EVA M. G. VIHO*, MAX GENTENAAR, LISA L. KOORNEEF, CEES VAN KOOTEN, PATRICK C. N. RENSEN, SANDER KOOIJMAN, HAZEL HUNT, ONNO C. MEIJER

**both authors contributed equally*

Pharmacol Res. 2021 Jun;168:105588.

ABSTRACT

Glucocorticoids regulate numerous processes in human physiology, but deregulated or excessive glucocorticoid receptor (GR) signaling contributes to the development of various pathologies including metabolic syndrome. For this reason, GR antagonists have considerable therapeutic value. Yet, the only GR antagonist that is clinically approved to date – mifepristone - exhibits cross-reactivity with other nuclear steroid receptors like the progesterone receptor. In this study, we set out to identify novel selective GR antagonists by combining rational chemical design with an unbiased *in vitro* and *in vivo* screening approach. Using this pipeline, we were able to identify CORT125329 as the compound with the best overall profile from our octahydro series of novel GR antagonists and demonstrated that CORT125329 does not exhibit cross-reactivity with the progesterone receptor. Further *in vivo* testing showed beneficial activities of CORT125329 in models for excessive corticosterone exposure and short- and long-term high-fat diet-induced metabolic complications. Upon CORT125329 treatment, most metabolic parameters that deteriorated upon high-fat diet feeding were similarly improved in male and female mice, confirming activity in both sexes. However, some sexually dimorphic effects were observed including male-specific antagonism of GR activity in brown adipose tissue and female-specific lipid lowering activities after short-term CORT125329 treatment. Remarkably, CORT125329 exhibits beneficial metabolic effects despite its lack of GR antagonism in white adipose tissue. Rather, we propose that CORT125329 treatment restores metabolic activity in brown adipose tissue by stimulating lipolysis, mitochondrial activity, and thermogenic capacity, although it is unclear if the regulation of these metabolic genes is mediated via direct GR antagonism in BAT. In summary, we have identified CORT125329 as a selective GR antagonist with strong beneficial activities in metabolic disease models, paving the way for further clinical investigation.

Key words: glucocorticoid receptor, glucocorticoids, high-fat diet, metabolic syndrome, mifepristone, selective antagonists

INTRODUCTION

Glucocorticoids are important regulators of energy homeostasis. In response to imbalance caused by either internal or external stimuli, the activation of the hypothalamic pituitary adrenal-axis results in the release of glucocorticoids into the bloodstream. The predominant endogenous glucocorticoid hormone is cortisol in humans, and corticosterone in mice. Glucocorticoids bind to the glucocorticoid receptor (GR, encoded by the *Nr3c1* gene), which is ubiquitously expressed in central and peripheral tissues and belongs to the nuclear receptor superfamily of ligand-dependent transcription factors. GR regulates the expression of many genes via transactivation and transrepression mechanisms [1]. GR and its target genes play an essential role in multiple physiological systems, including lipid and glucose metabolism. In addition, glucocorticoids are very well known for their immunosuppressive and anti-inflammatory properties [2].Because of these pleiotropic effects, deregulated or excessive GR signaling contributes to the development of numerous pathologies including the metabolic syndrome, mostly characterized by insulin resistance, glucose intolerance and dyslipidemia [3]. For this reason, GR antagonists have considerable therapeutic value [4]. Although this therapeutic strategy has received ample attention over the last decades, the only GR antagonist that is used in clinical practice is mifepristone (RU486) [5]. However, mifepristone lacks receptor selectivity [6], and its binding to the progesterone receptor underlies part of its side effects. The current use of mifepristone as GR antagonist is therefore largely limited to the treatment of patients with endogenous Cushing's syndrome [7].

To date, several novel GR antagonists are in clinical development. We previously described a series of *hexahydro*-1*H*-pyrazolo-isoquinolies as potent and selective GR antagonists [8]. Optimization of that series led to the discovery of CORT125134 (relacorilant) [8, 9]. This lead compound is currently under evaluation in Phase 3 clinical studies in patients with Cushing's syndrome and is being studied in combination with nab-paclitaxel in patients with ovarian and pancreatic cancer. Nevertheless, there is a clear need for a full spectrum of GR antagonists, exhibiting a range of properties allowing for their use in a variety of diseases involving GR signaling. In this study, we aimed to identify the most promising GR antagonists from our new *octahydro* series of compounds to counteract metabolic complications, using a complementary series of *in vitro* and *in vivo* models. Nine compounds that underwent initial *in vitro* screening are described below and two proceeded to further *in vitro* characterization and *in vivo* evaluation. Based on these results, the lead compound CORT125329 progressed to testing in metabolic disease models in

mice and was shown to prevent diet-induced metabolic complications in both male and female mice.

MATERIALS AND METHODS

1. HepG2 tyrosine aminotransferase activity assay

Human HepG2 cells were used to study tyrosine aminotransferase (TAT) activity, as previously described [8]. Cells were cultured in minimum essential medium supplemented with 10% fetal bovine serum, 2 mM L-glutamine and 1% nonessential amino acids. HepG2 cells were seeded at 25,000 cells per well and pre-treated with 3-10,000 nM test compounds for 30 min before addition of 100 nM dexamethasone. After 20 h, cells were lysed, and substrate mixture was added for 2 h before TAT activation was determined by measurement of light absorbance at 340 nm.

2. *In vitro* model for GR signaling in human HEK293T cells

Human HEK293T cells were used to study GR antagonism *in vitro*, as described previously [10]. Cells were cultured in DMEM-Glutamax supplemented with 10% charcoal-stripped fetal bovine serum and penicillin-streptomycin. HEK293T cells were seeded at 80,000 cells per well and transfected with 25 ng TAT1- or TAT3-firefly-luciferase reporter, 10 ng human GR or progesterone receptor (PR) expression vector, 1 ng CMV-renilla-luciferase reporter and 100 ng pcDNA using Fugene HD (Promega). Cells were pretreated with 0.1-1,000 nM mifepristone, CORT125522 or CORT125329 before exposure to 3 nM dexamethasone or 10 nM progesterone. After 24 h, firefly and renilla luciferase signals were measured using a dual-luciferase assay (Promega).

3. IL-6 production by human peripheral blood mononuclear cells

Human peripheral blood mononuclear cells (PBMCs) were isolated from a buffy coat of one healthy human donor by density gradient centrifugation using Ficoll isopaque. PMBCs were seeded at 150,000 cells per well in a 96-wells plate in RPMI supplemented with 10% charcoal-stripped FCS and penicillin-streptomycin. Cells were pretreated with 0.01-1000 nM mifepristone or CORT125329 for 1 h before 100 nM dexamethasone was added. After 24 h exposure to dexamethasone, PBMCs were stimulated with 100 ng/ml lipopolysaccharide (LPS, Enzo Life Sciences) for 6 h and supernatant was collected to determine human IL-6 levels by ELISA according to manufacturer's protocol (Sanquin M9316).

4. Animal studies

All animal studies were approved by the ethics committee of Leiden University Medical Center. C57Bl/6J mice (Charles River) were group-housed in conventional cages with a 12:12 h light-dark cycle and had *ad libitum* access to food and water.

4.1. Sub-chronic corticosterone model

In our model for sub-chronic corticosterone exposure [11], we performed *in vivo* screening experiments in 8-week-old male C57Bl/6J mice subcutaneously implanted with corticosterone-releasing pellets (12.5 mg corticosterone, Sigma, 87.5 mg cholesterol, BioChemica) under isoflurane anesthesia. Mice were treated by oral gavage with 60 mg/kg/day mifepristone (N=6), CORT125329 (N=6), CORT125522 (N=6) or solvent (N=6; 10% DMSO, 0.1% Tween-80, 0.5% hydroxypropyl methylcellulose in PBS) for 5 days.

In a follow-up experiment, we investigated 120 mg/kg/day CORT125329 (N=8) and compared this to 60 mg/kg/day mifepristone treatment (N=3) and solvent treatment (N=6). Body weight and composition (by echo-MRI) were determined at baseline (3 days prior to treatment and pellet-implantation) and at day 5 of treatment. Blood was collected after a 6 h fast at baseline and at day 5 of treatment for analysis of plasma biochemistry and total white blood cell count (Sysmex XT-2000iV). Mice were killed by CO2 asphyxiation and tissues of interest were collected and snap-frozen until further analysis.

4.2. Short- and long-term high-fat diet models

In our short-term model for diet-induced obesity and metabolic disease, we performed the same experiment in 8-week-old male and female C57Bl/6J mice. These were fed with 60% high-fat diet (HFD) and 10% fructose water for 14 days. Mice were treated daily by oral gavage with solvent (PBS with 10% DMSO, 0.1% Tween-80 and 0.5% hydroxypropyl methylcellulose) (N=12; of which N=6 for vehicle injection at endpoint and N=6 dexamethasone-phosphate injection at endpoint), 60 mg/kg mifepristone (N=6; dexamethasone-phosphate injection at endpoint) or 120 mg/kg CORT125329 (N=6; dexamethasone-phosphate injection at endpoint). Body weight and composition (echo-MRI) were determined twice a week, and blood was collected after a 6 h fast at baseline, day 7 and day 14 to determine plasma biochemistry (glucose, insulin, triglycerides, and total cholesterol). An oral glucose tolerance test was performed at day 7. After a 6 h fast, 1 g/kg glucose was administered by oral gavage and blood was collected at t=5, 30, 60 and 120 min to determine glucose and insulin levels. At day 14, 1 h after the last treatment with vehicle, mifepristone or CORT125329, mice were subcutaneously injected with 5

mg/kg dexamethasone-phosphate (Merck, dissolved in PBS) or vehicle, and 6 h after injection mice were killed by CO2 asphyxiation to collect tissues of interest.

In our long-term model for diet-induced obesity and metabolic disease, 8-week-old male C57Bl/6J mice were fed with 60% HFD and 10% fructose water for 50 days, and this was compared to low-fat diet (LFD). Under HFD, mice were treated with 60 or 120 mg/kg/day CORT125329 via diet-supplementation, in a preventive or therapeutic treatment regimen (N=8 mice per group). Mice in the preventive treatment groups received diet supplemented with CORT125329 from the beginning of the experiment at day 0, while mice in the therapeutic treatment group first received a HFD run-in diet for 3 weeks after they received CORT125329-supplemented HFD from day 21 onwards. Body weight and composition (echo-MRI) were determined weekly, and blood was collected after a 6 h fast at baseline, day 21 and day 42 to determine plasma biochemistry (glucose, insulin, triglycerides, free fatty acids, and total cholesterol). An oral glucose tolerance test was performed at day 42. After a 6 h fast, 1 g/kg glucose was administered by oral gavage and blood was collected at t=5, 10, 15, 30, 60 and 120 min to determine glucose and insulin levels. At day 50, nutrient clearance from the circulation was assessed.

To this end, mice were fasted for 6 h and intravenously injected with [^{14}C] deoxyglucose and 80 nm triglyceride-rich lipoprotein-like emulsion particles labeled with glycerol tri-[^{3}H] oleate [12]. Blood was collected at t=0, 2, 5, 10 and 15 min after injection. Mice were killed by CO2 asphyxiation, perfused with ice-cold PBS for 5 min and tissues of interest were collected. In plasma and tissue samples, [^{3}H] and [^{14}C] activity were measured by liquid scintillation.

5. Plasma biochemistry

Plasma samples were analyzed for triglyceride and cholesterol levels (both enzymatic kits from Roche Diagnostics), free fatty acids and glucose (both kits from Wako Diagnostics) and insulin (Crystal Chem), all according to manufacturer's instructions. The homeostatic model assessment for insulin resistance (HOMA-IR) was calculated by multiplying the fasted glucose concentration (mmol/l) with the fasted insulin concentration (mmol/l).

6. RNA isolation, cDNA synthesis and real-time quantitative PCR

Total RNA was isolated from snap-frozen liver, interscapular brown adipose tissue (iBAT) and gonadal white adipose tissue (gWAT) samples using TriPure Isolation reagent (Roche). 1 µg mRNA was used for cDNA synthesis using M-MLV reverse

transcriptase (Promega). Gene expression was assessed by real-time quantitative PCR using IQ SYBR-Green supermix and a MyIQ Thermal Cycler (Bio-Rad CFX96).

7. Protein isolation and western blot analysis

Western blot on a subset of iBAT samples (N=4 per group) was performed using the WES (ProteinSimple). The following primary antibodies were used: goat-anti-mouse lipoprotein lipase (LPL; in house antibody, 1:50 dilution), rabbit-anti-mouse uncoupling protein-1 (UCP1; Sigma U6382, 1:20 dilution), rabbit-anti-mouse tubulin (Cell Signaling 2148, 1:20 dilution).

8. Statistical analysis

All data are expressed as mean ± sem. Statistical significance was calculated using GraphPad Prism 8 using a one-way or 2-way ANOVA as indicated in the figure legends.

RESULTS

Pipeline for identification and characterization of novel GR antagonists

We set out to develop and characterize novel GR antagonists by introducing a minor modification (saturation of the central ring) to the original hexahydro series, which provided a second promising series: the octahydro series. In general, the octahydro series tended to be less potent as GR antagonists compared to the corresponding hexahydro-based compounds. Nevertheless, CORT125281 was identified from the octahydro series [8] as a potent GR antagonist *in vivo* [11, 13]. Within the octahydro series, our goal was the identification of additional compounds and those were initially selected due to their good potency as GR antagonists (Ki < 20nM in our functional TAT assay) combined with a good oral pharmacokinetic profile in rats (data not shown). Compounds that passed these initial criteria were fed into our pipeline for novel GR antagonists that encompasses *in vitro* pharmacology, *in vivo* screening, and evaluation in metabolic disease models (**Fig. 1**).

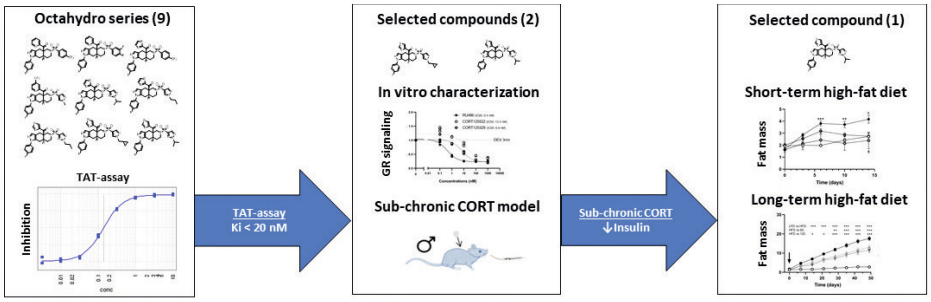

Figure 1. Schematic overview of the workflow for evaluation of the octahydro series, including criteria for selection, *in vitro* and *in vivo* models and number of compounds in each stage. Abbreviations: CORT = corticosterone, GR = glucocorticoid receptor, TAT = tyrosine amino transferase.

Chemical modification of the octahydro series and initial evaluation of GR antagonism *in vitro*

The exploration of the octahydro series focused on varying the nature of the heteroaryl ketone, and the sulphonamide substituent. Initially we incorporated an unsubstituted 2-pyridyl ketone, exemplified by compounds **1** and **2** (**Fig. 2**). However, as noted previously in the hexahydro series, compounds with this substituent did not provide adequate potency. Replacing the 2-pyridyl with 2-thiazolyl had little effect on potency, as shown by compound **3**. Based on the structure activity relationships previously defined in the hexahydro series, we added a trifluoromethyl substituent to the pyridyl, and replaced the substituted phenyl sulphonamide by a substituted pyrazole sulphonamide, as shown by compound **4**. This compound is the direct analogue of CORT125134 in the hexahydro series but has substantially lower potency. In the presence of a heteroaryl sulphonamide, either pyrazole or triazole, the trifluoromethylpyridyl can be replaced by a 2-thiazolyl ketone – compounds **5** and **6** possess moderate potency, similar to compound **4**.

Attachment of the thiazole via the 4-position, rather than the 2-position, provided several interesting compounds including **7**, **8** and **9**. Compound **8** (CORT125522) and compound **9** (CORT125329) were evaluated in pharmacokinetic studies in rats and both compounds provided high bioavailability and excellent plasma concentrations after oral dosing (data not shown).

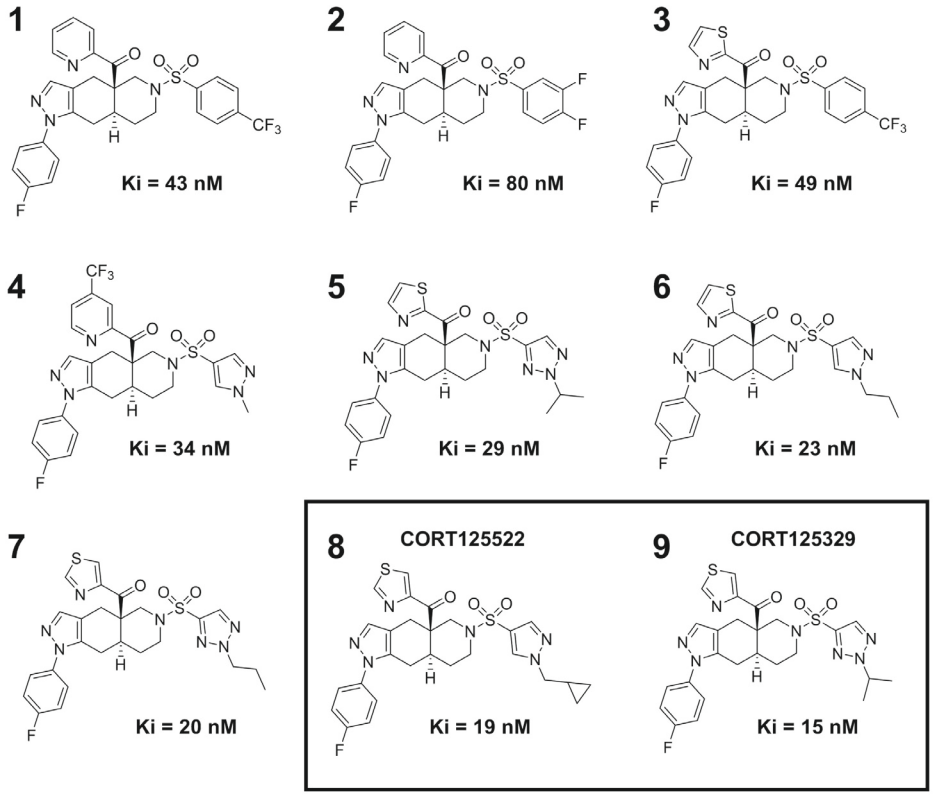

Figure 2. Chemical structures of 9 compounds of the octahydro series, including CORT125522 and CORT125329. The inhibitor constant (Ki) for each compound was determined in the HepG2 tyrosine amino transferase (TAT) assay.

Based on this, we selected CORT125522 and CORT125329 for further evaluation. CORT125522 and CORT125329 potently inhibited dexamethasone-induced GR transactivation in human HEK293T cells, albeit the IC50 of these novel GR antagonists was approximately >20 to 30-fold higher as compared to mifepristone (**Fig. 3A**). Although mifepristone exhibits PR cross-reactivity, we demonstrate that both CORT125522 and CORT125329 are completely devoid of this activity (**Fig. 3B**). CORT125552 and CORT125329 exhibit antagonism of anti-inflammatory activity, as the inhibitory effect of dexamethasone on LPS-induced IL-6 release was completely prevented by pre-treatment with 1 μM of these compounds (**Fig. 3C**). Based on these promising *in vitro* observations, we proceeded to further *in vivo* evaluation with CORT125522 and CORT125329.

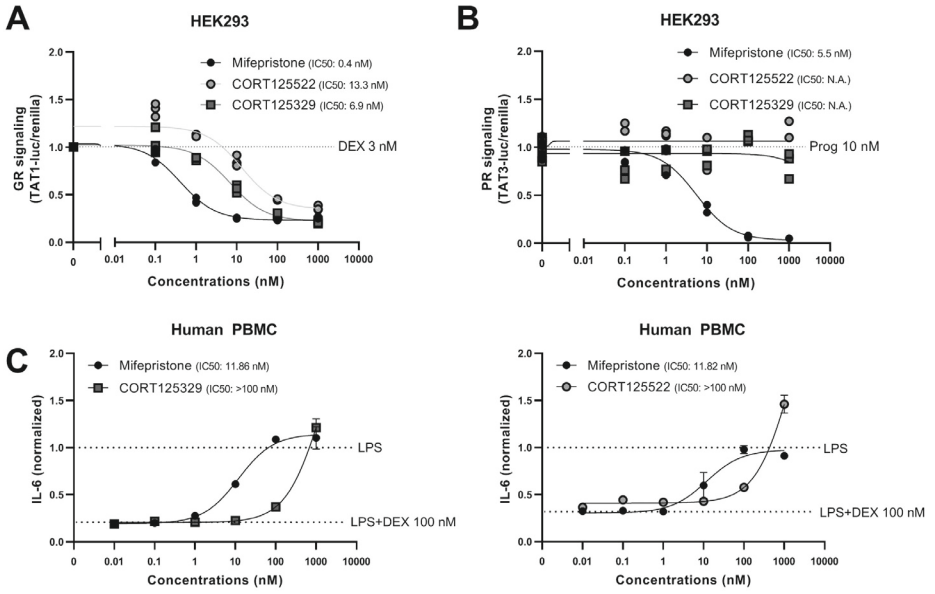

Figure 3. *In vitro* characterization of 2 selected compounds, CORT15522 and CORT125329. The effect of mifepristone, CORT125522 and CORT125329 on **(A)** dexamethasone-induced GR transactivation and **(B)** progesterone-induced PR transactivation in human HEK293T cells. **(C)** The effect of mifepristone, CORT125522 and CORT125329 on dexamethasone-suppressed LPS-stimulated IL-6 secretion in human peripheral blood mononuclear cells (PBMC). Abbreviations: DEX = dexamethasone, GR = glucocorticoid receptor, PR = progesterone receptor, LPS = lipopolysaccharide, TAT = tyrosine amino transferase.

CORT125329 partially prevents excess corticosterone-induced symptoms

In our *in vivo* follow-up (**Fig. 4A**), we sub-chronically exposed male C57Bl/6J mice to elevated corticosterone levels to evaluate the effect of daily treatment with CORT125522 and CORT125329 in comparison with the benchmark GR antagonist mifepristone. In line with our previous findings [11], sub-chronic corticosterone exposure rapidly results in immune suppression (**Fig. 4B**) and hyperinsulinemia (**Fig. 4C**). As expected, daily treatment with mifepristone completely prevented corticosterone-induced leukopenia ($p<0.001$, **Fig. 4B**) and hyperinsulinemia ($p<0.01$, **Fig. 4C**), resulting in a normalized HOMA-IR index ($p<0.05$, **Fig. 4D**). Treatment with CORT125522 and CORT125329 at a dose of 60 mg/kg/day did not influence corticosterone-induced leukopenia (**Fig. 4B**). CORT125329 seemed to lower corticosterone-induced insulin levels and decreased the HOMA-IR at trend level ($p=0.08$, **Fig. 4D**). As CORT125522 treatment did not influence WBC, insulin, and HOMA-IR (**Fig. 4B-D**), it was omitted for further analysis.

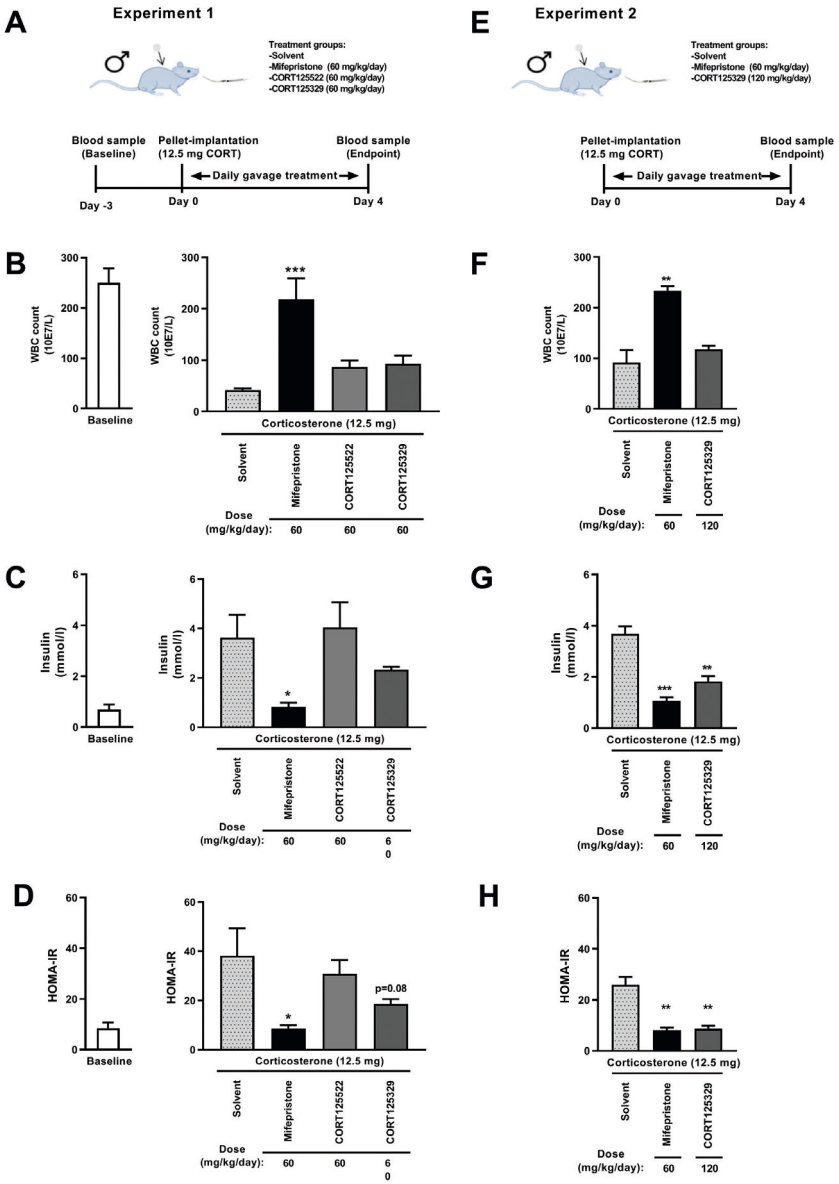

Figure 4. *In vivo* activity of 2 selected compounds CORT125329 and CORT125522 in male C57Bl/6J mice with sub-chronic corticosterone exposure. (A) Outline of experiment 1. **(B)** Total white blood cell count (WBC), **(C)** insulin levels and **(D)** HOMA-IR of mice at baseline and at endpoint after exposure to corticosterone-pellets and treatment with either solvent, mifepristone, CORT125522 or CORT125329 (all 60 mg/kg/day). **(E)** Outline of experiment 2. **(F)** WBC, **(G)** insulin and **(H)** HOMA-IR of mice at baseline and at endpoint after treatment with solvent, 60 mg/kg/day mifepristone or 120 mg/kg/day CORT125329. Statistical differences were calculated using a one-way ANOVA with Dunnett's multiple comparisons test. * $p<0.05$ vs. solvent, ** $p<0.01$ vs solvent, *** $p<0.001$ vs solvent. Abbreviations: CORT = corticosterone, WBC = white blood cell count.

We followed up on CORT125329 in this model by evaluating its effects at the higher dose of 120 mg/kg/day (**Fig. 4E**). Although this did not influence the corticosterone-induced effects on WBC (**Fig. 4F**), treatment with 120 mg/kg/day CORT125329 significantly lowered insulin levels ($p<0.01$, **Fig. 4G**) and decreased the HOMA-IR ($p<0.01$, **Fig. 4H**), comparable to the effect of mifepristone treatment. As we previously observed tissue-specific activities of certain GR antagonists [11], we investigated the ability of CORT125329 to inhibit corticosterone-induced GR-target gene expression in liver, iBAT and gWAT. In our model for sub-chronic corticosterone exposure, CORT125329 treatment lowered the expression of *Fkbp5*, *Gilz* and *Mttp* in the liver (**Suppl. Fig 1A**), and *Fkbp5* and *Gilz* in iBAT (**Suppl. Fig. 1B**) but did not affect gene expression in gWAT (**Suppl. Fig 1C**), revealing a tissue-specific pattern of GR antagonism by CORT125329.

CORT125329 reduces short-term HFD-induced metabolic dysfunction in male and female mice

As CORT125329 showed beneficial metabolic properties in our excess corticosterone model, we investigated if CORT125329 has utility in a short-term HFD study. Because the development of metabolic disease and GR signaling are often sex-dependent, we tested the activity of CORT125329 in both male and female C57Bl/6J mice. In both sexes, HFD-feeding for 14 days resulted in increased total body weight and fat mass as compared to LFD (**Fig. 5A-B**). Daily treatment with CORT125329 largely prevented HFD-induced body weight gain in both sexes reaching statistical significance in female mice ($p<0.001$, **Fig. 5A**), and attenuated HFD-induced fat mass gain in both sexes (**Fig. 5B**). Mifepristone treatment non-significantly lowered body weight and fat mass in male mice, and significantly decreased body weight and fat mass in female mice (**Fig. 5A-B**).

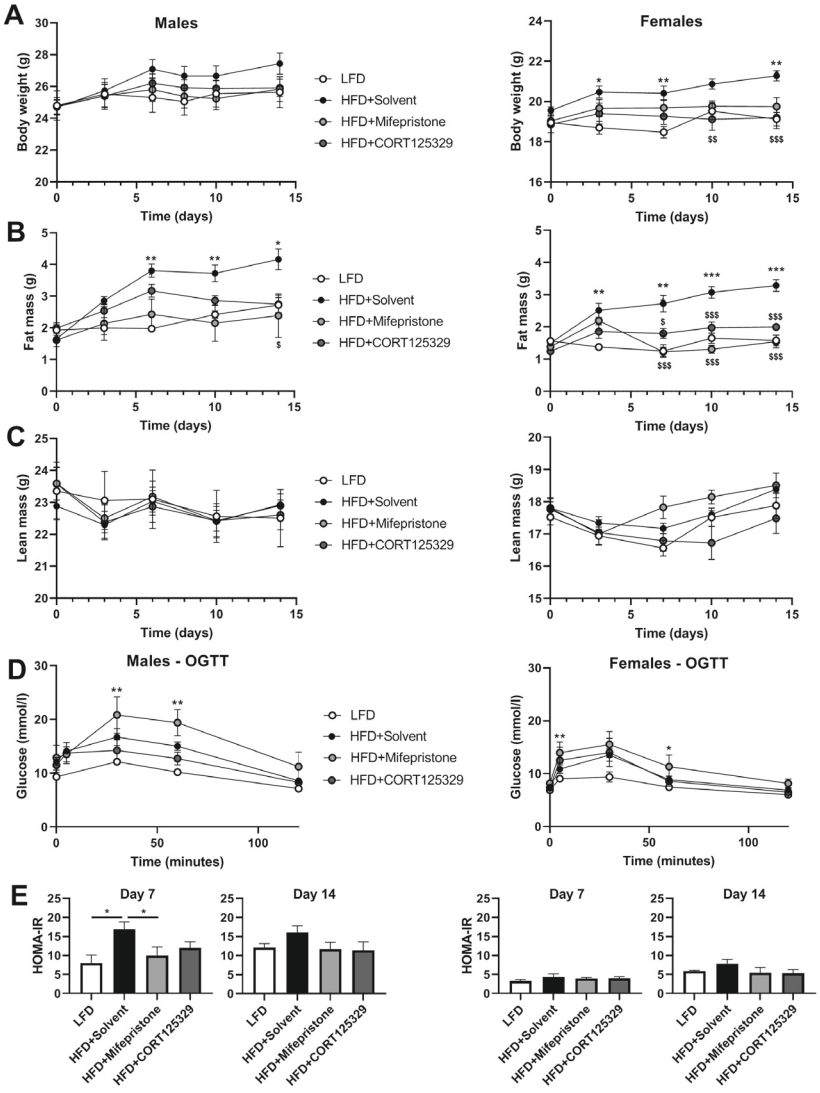

Figure 5. The effect of CORT125329 in male and female mice with short-term exposure to high-fat diet. The effect of daily solvent, mifepristone or CORT125329 treatment on **(A)** body weight, **(B)** fat mass and **(C)** lean mass of male and female mice under high-fat diet exposure. Statistical differences were calculated using a 2-way ANOVA with Tukey's multiple comparisons test. *p<0.05 vs LFD, **p<0.01 vs LFD, ***p<0.001 vs LFD, $ p<0.05 vs HFD+Solvent, $$ p<0.01 vs HFD+Solvent, $$$ p<0.001 vs HFD+Solvent. **(D)** The effect of daily solvent, mifepristone or CORT125329 treatment on glucose levels during an oral glucose tolerance test in male and female mice. Statistical differences were calculated using a 2-way ANOVA with Dunnett's multiple comparisons test. *p<0.05 vs HFD+Solvent, **p<0.01 vs HFD+Solvent. **(E)** The effect of daily solvent, mifepristone or CORT125329 treatment on HOMA-IR (homeostatic model assessment for insulin resistance) at day 7 and 14. Statistical differences were calculated using a one-way ANOVA with Dunnett's multiple comparisons test. *p<0.05. Abbreviations: LFD = low-fat diet, HFD = high-fat diet.

In both male and female mice, lean mass was not affected by HFD-feeding nor mifepristone or CORT125329 treatment (**Fig. 5C**). We next analyzed oral glucose tolerance of HFD-fed mice treated with vehicle, mifepristone and CORT125329. Under HFD conditions, CORT125329 did not significantly change glucose tolerance in male and female mice (**Fig. 5D**). In contrast to our expectation, mifepristone significantly increased glucose levels during the glucose tolerance test (**Fig. 5D**). In male mice, mifepristone treatment significantly lowered the HOMA-IR index at day 7, while CORT125329 treatment non-significantly decreased this (**Fig. 5E**). In female mice, HOMA-IR was only modestly increased upon HFD-feeding but seemed lowered after 14 days of mifepristone and CORT125329 treatment (**Fig. 5E**). The lower HOMA-IR index was mainly a result of reduced plasma insulin levels that were observed after mifepristone and CORT125329 treatment (**Suppl. Fig. 2A**), while glucose levels were not altered upon HFD-feeding nor mifepristone or CORT125329 treatment (**Suppl. Fig. 2B**). A noteworthy sex difference that we observed is that CORT125329 strongly reduced plasma levels of triglycerides and cholesterol in female mice after 14 days, while no effects were observed in male mice at this time point (**Suppl. Fig. 2C-D**). At endpoint, male and female mice were injected with dexamethasone to activate the GR. This revealed that female BAT was more sensitive to GR activation by dexamethasone, as the induction of GR-responsive genes was much stronger in female mice as compared to male mice (38-fold induction of *Fkbp5* expression in male BAT as compared to a 135-fold induction in female BAT; 4-fold induction of *Gilz* expression in male BAT as compared to a 12-fold induction in female BAT; **Suppl. Fig. 3**). Treatment with both mifepristone and CORT125329 attenuated dexamethasone-induced expression of *Fkbp5* and *Gilz* in BAT of male mice, but not in female mice (**Suppl. Fig. 3**). Altogether, CORT125329 treatment improved metabolic health in both male and female mice but exhibits sex differences in GR antagonism in BAT and in plasma lipid levels.

CORT125329 treatment alleviates long-term HFD-induced metabolic dysfunction

Given the efficacy of CORT125329 in our short-term HFD study, we next investigated CORT125329 in a long-term model of HFD-induced metabolic dysfunction in male C57Bl/6J mice. In this study, we evaluated different treatment regimens, *i.e.*, different doses (60 and 120 mg/kg/day) and preventive treatment versus therapeutic treatment. HFD-feeding rapidly induced an increase in body weight and fat mass, while lean mass was not affected during the 7 weeks experimental period (**Fig. 6A-C**). In a preventive treatment regimen, both 60 and 120 mg/kg/day doses of CORT125329 significantly decreased HFD-induced body weight gain and fat mass (**Fig. 6A-B, left panels**).

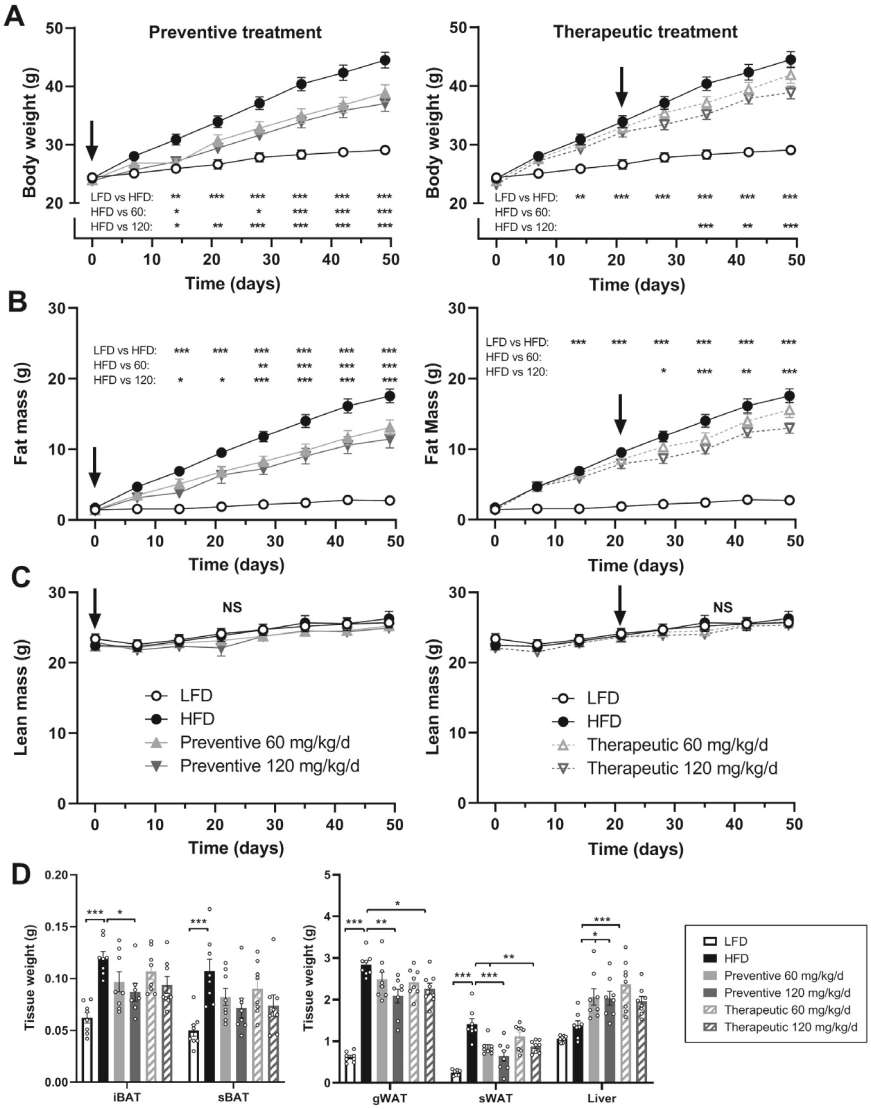

Figure 6. The effect of CORT125329 on body weight, body composition and metabolic tissue weights in male mice with long-term exposure to high-fat diet. The effect of preventive (left) or therapeutic treatment regimens (right) with CORT125329 on **(A)** body weight, **(B)** fat mass and **(C)** lean mass under high-fat diet exposure. Start of treatment is indicated with an arrow; LFD and HFD control groups plotted in preventive and therapeutic graphs are the same. Statistical differences were calculated using a 2-way ANOVA with Tukey's multiple comparisons test. **(D)** Wet tissue weight of interscapular brown adipose tissue (iBAT), subscapular brown adipose tissue (sBAT), gonadal white adipose tissue (gWAT), subcutaneous white adipose tissue (sWAT) and liver. *p<0.05, **p<0.01, ***p<0.001, NS=non-significant. Abbreviations: HFD = high-fat diet, LFD = low-fat diet.

In a therapeutic treatment regimen, only 120 mg/kg/day CORT125329 significantly lowered body weight gain and fat mass (**Fig. 6A-B, right panels**). Both doses of CORT125329 and both regimens did not influence lean body mass (**Fig. 6C, left and right panel**).

Postmortem analysis of tissues showed that HFD increased the wet weight of iBAT, sBAT, gWAT and sWAT (**Fig. 6D**). iBAT tissue weight was significantly decreased by preventive treatment with 120 mg/kg/day CORT125329 (**Fig. 6D**). gWAT tissue weight was decreased by preventive and therapeutic treatment with 120 mg/kd/day CORT125329, and sWAT weight was decreased by 60 and 120 mg/kg/day preventive treatment and 120 mg/kg/day therapeutic treatment (**Fig. 6D**). Of note, liver weight was non-significantly increased by HFD feeding as compared to LFD and was further increased by CORT125329 in all treatment settings (**Fig. 6D**). HFD-feeding severely compromised glucose metabolism, resulting in hyperinsulinemia (**Suppl. Fig. 4A**), reduced insulin sensitivity (**Fig. 7A-B**), delayed plasma clearance of an intravenously injected [^{14}C] deoxyglucose tracer (**Suppl. Fig. 5A**) and decreased [^{14}C] deoxyglucose uptake by iBAT, sBAT and sWAT (**Fig. 7C**). Both preventive and therapeutic treatment with 60 and 120 mg/kg/day CORT125329 reduced HFD-induced hyperinsulinemia ($p<0.001$), resulting in an improved HOMA-IR ($p<0.001$ for 60 and 120 mg/kg/day preventive treatment, $p<0.01$ for 120 mg/kg/day therapeutic treatment, **Suppl. Fig. 4A**). In an oral glucose tolerance test, both preventive and therapeutic treatment with 60 and 120 mg/kg/day CORT125329 lowered the glucose excursion and insulin levels (**Fig. 7A**), resulting in a significantly lower area under the curve for both glucose and insulin (**Fig. 7B**). Preventive treatment with 60 and 120 mg/kg/day and therapeutic treatment with 120 mg/kg/day restored rapid clearance of intravenously injected [^{14}C] deoxyglucose from plasma upon HFD-feeding (**Suppl. Fig. 5A**). For all the tissues that were assessed, uptake of [^{14}C] deoxyglucose was unaltered upon CORT125329 treatment (**Fig. 7C**).

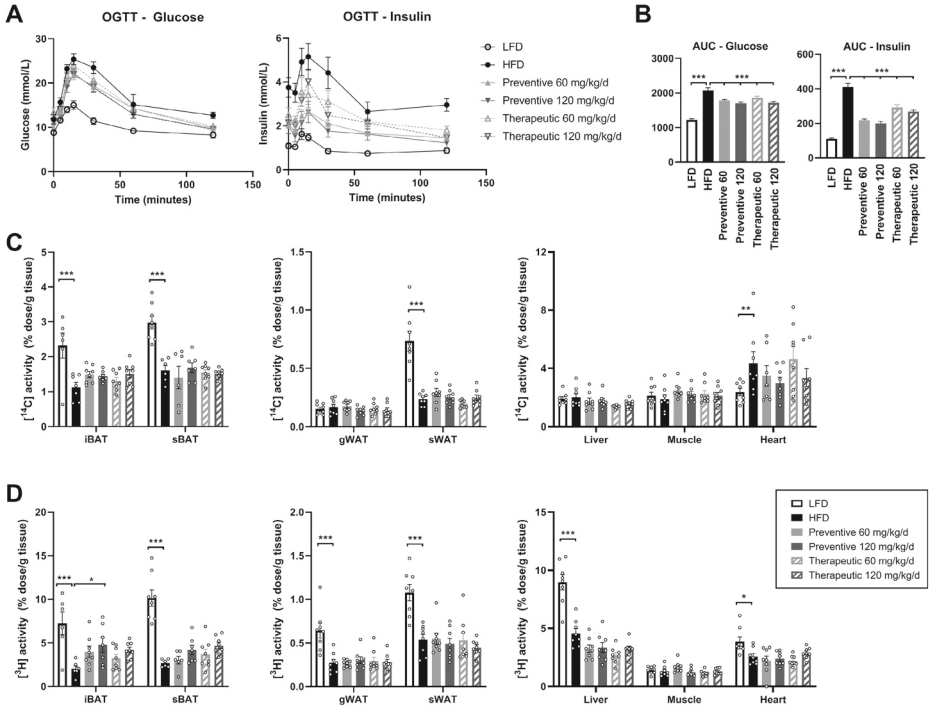

Figure 7. The effect of CORT125329 on glucose and lipid metabolism in male mice with long-term exposure to high-fat diet. (A) Glucose and insulin levels and **(B)** area under the curve during an oral glucose tolerance test. **(C)** Tissue-specific uptake of [^{14}C] deoxyglucose and **(D)** [^{3}H] oleate. Statistical differences were calculated using a one-way ANOVA with Tukey's multiple comparisons test. *p<0.05, **p<0.01, ***p<0.001. Abbreviations: AUC = area under the curve, HFD = high-fat diet, LFD = low-fat diet, OGTT = oral glucose tolerance test.

We next investigated the effect of CORT125329 on lipid metabolism. Plasma levels of triglycerides and free fatty acids were unaltered by HFD and were decreased by preventive and therapeutic treatment with CORT125329 (**Suppl. Fig. 4B**). HFD increased plasma cholesterol levels, which was lowered by both preventive and therapeutic treatment with CORT125329 (**Suppl. Fig. 4B**). Furthermore, HFD delayed clearance of glycerol tri-[^{3}H] oleate-labeled lipoprotein-like particles from plasma, which recovered upon CORT125329 treatment (**Suppl. Fig. 5B**). Finally, HFD significantly lowered [^{3}H] oleate uptake by iBAT, sBAT, gWAT, sWAT, liver and heart as compared to LFD. Preventive treatment with 120 mg/kg/day CORT125329 partially improved [^{3}H] oleate uptake by iBAT, but not by other tissues (**Fig. 7D**).

Long-term CORT125329 treatment alters BAT activity under HFD conditions
The increased uptake of [^{3}H] oleate and the tendency towards enhanced [^{14}C] deoxyglucose uptake by BAT, and the decreased wet tissue weights collectively suggests increased metabolic and thermogenic activity upon CORT125329 treatment.

Gene expression analysis of iBAT revealed that many metabolic pathways were deregulated by HFD-feeding and partially normalized after CORT125329 treatment, including those involved in lipid uptake, thermogenesis, lipolysis, glucose uptake, lipogenesis, mitochondrial activity and glycolysis (**Fig. 8A-G**). Under HFD-feeding, CORT125329 treatment non-significantly increased expression of *lipoprotein lipase* (*Lpl*) mRNA and LPL protein, which is involved in triglyceride-derived fatty acid uptake by BAT (**Fig. 8A, Suppl. Fig. 6**).

Thermogenic protein UCP1 was strongly and significantly increased by therapeutic CORT125329 treatment under HFD-feeding conditions (**Fig. 8B, Suppl. Fig. 6**). Lipolysis markers *adipose triglyceride lipase* (*Atgl*) and *hormone sensitive lipase* (*Hsl*) were significantly upregulated by both doses of CORT125329 in both treatment regimens, as compared to HFD alone (**Fig. 8C**). Although *glucose transporter type 1* (*glut1*) expression was not altered by HFD or CORT125329 treatment, the expression of *glucose transporter type 4* (*Glut4*) was upregulated by CORT125329 treatment (**Fig. 8D**). As for lipogenesis activity, therapeutic treatment with 120 mg/kg/day CORT125329 resulted in increased expression of *diacylglycerol acyltransferase 2* (*Dgat2*), *fatty acid synthase* (*Fasn*) and *acetyl-CoA carboxylase 1* (*Acc1*), while *acetyl-CoA carboxylase 2* (*Acc2*) gene expression was enhanced by all CORT125329 treatment groups, as compared to HFD (**Fig. 8E**). Finally, CORT125329 treatment elevated expression of two genes involved in mitochondrial activity: *peroxisome proliferator-activated receptor gamma* (*Pparg*) and *citrate synthase* (*Cs*) (**Fig. 8F**), and the glycolysis gene *hexokinase 2* (*Hk2*) (**Fig. 8G**), but did not influence the *peroxisome proliferator-activated receptor gamma coactivator 1-alpha* (*Pgc1a*) expression (**Fig. 8F**), as compared to HFD. CORT125329 treatment thus restores HFD-induced deregulation of metabolic pathways in BAT.

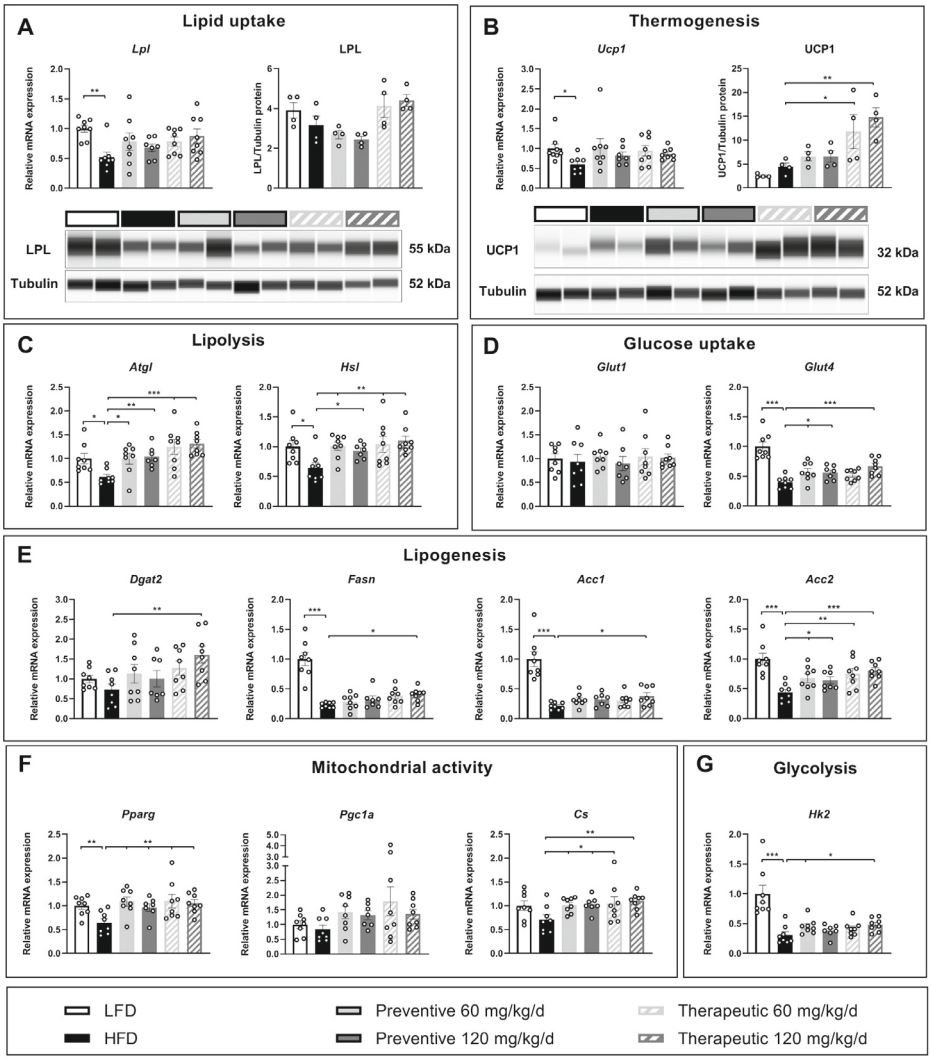

Figure 8. The effect of CORT125329 on metabolic pathways in brown adipose tissue. The effect of preventive or therapeutic treatment with 60 and 120 mg/kg/day CORT125329 under high-fat diet exposure on interscapular brown adipose tissue mRNA and protein expression of markers involved in **(A)** lipid uptake and **(B)** thermogenesis. mRNA expression of genes involved in **(C)** lipolysis, **(D)** glucose uptake, **(E)** lipogenesis, **(F)** mitochondrial activity and **(G)** glycolysis. Statistical differences were calculated using a one-way ANOVA with Dunnett's multiple comparisons test. *p<0.05, **p<0.01, ***p<0.001.

DISCUSSION

In this study, we set out to identify novel GR antagonists by combining rational chemical design with an unbiased *in vitro* and *in vivo* screening approach. Using this pipeline, we were able to identify CORT125329 as the compound with the best overall profile from our octahydro series of novel GR antagonists. Out of the nine compounds of this series that are described in this article, CORT125329 exhibited the lowest Ki in the initial HepG2 TAT-assay and was therefore taken forward for further testing together with CORT125522. The evaluation of these compounds confirmed antagonism on dexamethasone-induced GR transactivation. Further downstream in our pipeline, we found that CORT125329 was superior to CORT125522 treatment in preventing corticosterone-induced hyperinsulinemia. Despite its ability to overcome the anti-inflammatory activity of dexamethasone in human PBMCs, *in vivo* treatment with CORT125329 was insufficient to prevent the immune-suppressive effects of prolonged overexposure to corticosterone. This discrepancy may be dose related – *ex vivo* effects of dexamethasone on human PMBCs were prevented by CORT125329 only in a micromolar range – and sufficient concentrations of CORT125329 may not be reached *in vivo* in immune tissues like the bone marrow, spleen, and thymus. In line with this, CORT125329 treatment of male mice was insufficient to overcome the decreased thymus and spleen weight upon excessive corticosterone exposure (data not shown).

The activity of CORT125329 was further evaluated in additional metabolic disease models. In a short-term HFD study, CORT125329 was tested in a direct comparison with mifepristone. Albeit at a higher dose, CORT125329 performed similarly to mifepristone in attenuating HFD-induced body weight, fat mass gain and hyperinsulinemia. We did not find a strong improvement of glucose tolerance by CORT125239 treatment upon short-term HFD exposure as mice were still relatively glucose tolerant, but we did observe restored glucose tolerance in long-term HFD exposed mice after prolonged CORT125329 treatment. Altogether, CORT125329 thus exhibits clear beneficial activities in HFD-induced metabolic disease and performs similarly to the benchmark GR antagonist mifepristone in preventing corticosterone-induced hyperinsulinemia.

Glucocorticoid-associated metabolic effects can be – and often are - sex-dependent [14–18]. Many aspects of the metabolic syndrome that predispose for the development of cardiovascular diseases are either more pronounced in men or more common in women, and the hormonal profile is often suggested as an important contributor to this sex difference [19]. Moreover, the most commonly

used GR antagonist mifepristone exhibits strong cross-reactivity to other hormone receptors, most notably the progesterone receptor [13, 20]. Despite these well-documented properties, many studies on GR antagonists or modulators – including many of our own – used exclusively male animals [11, 13, 21–24]. In the current study we addressed this caveat by performing key experiments in both male and female mice. Our results suggest that CORT125329 treatment reduced HFD-induced body weight gain, fat mass gain and hyperinsulinemia similarly in male and female mice.

Although we observed lipid lowering properties of CORT125329 in male mice after long-term treatment, CORT125329 treatment up to two weeks only lowered plasma triglycerides and cholesterol in female mice but not male mice. These differences confirm the notion that one should consider investigating the effect of GR antagonism in both sexes as sexually dimorphic effects may exist in treatment response. It is important to note that CORT125329 exhibits tissue-specific activity – which may even be dependent on sex (*i.e.*, GR antagonism in male but not female BAT). In male mice, CORT125329 has potent GR antagonism in brown adipose tissue, but no GR antagonism in white adipose tissue, similar to the recently described GR antagonist CORT125281 [11]. It is therefore unclear via which (combination of) tissue(s) CORT125329 exerts its beneficial effects on metabolism, although direct effects on white adipose tissue are unlikely. We could partially exclude the hypothesis of cell-specific GR antagonism in white adipose tissue, as we observed no effects by CORT125329 on the expression of adipocyte-specific GR-regulated gene *adiponectin* and of the endothelial-specific gene *Cdh5*. It was previously reported that dexamethasone-induced hyperinsulinemia and insulin resistance is dependent on (brown) adipocyte GR, but that the development of HFD-induced hyperinsulinemia is independent of adipocyte GR expression [25]. Given the observation that CORT125329 treatment did not influence GR signaling in WAT, it seems that the improved metabolic phenotype is thus independent of adipose tissue GR expression, but rather mediated via GR antagonism in other tissues like liver, pancreas and/or skeletal muscle that can release a variety of endocrine factors to regulate distant tissues like BAT. There are indications that BAT activity is increased upon CORT125329 treatment, as we observe decreased BAT tissue weights (indicative of enhanced thermogenic activity), elevated uptake of [^{3}H] oleate and a non-significant increase in [^{14}C] deoxyglucose uptake. In addition to this, our molecular analysis revealed that CORT125329 treatment restored the activity of many downstream metabolic pathways in BAT that were disturbed upon HFD-feeding. Elevated LPL expression upon CORT125329 treatment can underlie the increased triglyceride-derived fatty acid uptake in BAT, while elevated [^{14}C] deoxyglucose uptake was mirrored by increased expression of glucose transporter

Glut4. CORT125329 treatment readily upregulated UCP1 protein expression, indicating increased thermogenic activity. As mentioned before, it is unclear if the regulation of these metabolic genes is the direct effect of GR antagonism in BAT, or if other endocrine tissues respond to CORT125329 treatment that subsequently influence BAT activity. In addition to tissue-specific properties, CORT125329 may also exhibit cell type-specific effects within a single tissue. A recent study using single nuclei RNA-sequencing shows a striking heterogeneity in adipocyte identity within mouse BAT and revealed a rare subpopulation of adipocytes that increases in abundance at high temperatures and regulates the activity of other adipocytes in their proximal neighbourhood through acetate-mediated modulation of their thermogenic capacity [26]. Such populations may differ in GR expression. We exclusively used bulk tissue for our expression analysis that does not allow us to capture cell type-specific effects, but CORT125329 activity could be mediated via activities on specific cellular subtypes present within BAT.

In conclusion, we identified a novel specific GR antagonist – CORT125329 – that antagonizes GR in a tissue-specific manner and improves metabolic health in several disease models via activation of BAT. Our promising preclinical data with CORT125329 warrant further clinical evaluation in humans.

REFERENCES

1. Quatrini, L. and S. Ugolini, *New insights into the cell- and tissue-specificity of glucocorticoid actions.* Cell Mol Immunol, 2020.
2. Moraitis, A.G., et al., *The role of glucocorticoid receptors in metabolic syndrome and psychiatric illness.* J Steroid Biochem Mol Biol, 2017. **165**(Pt A): p. 114-120.
3. Kadmiel, M. and J.A. Cidlowski, *Glucocorticoid receptor signaling in health and disease.* Trends Pharmacol Sci, 2013. **34**(9): p. 518-30.
4. Diaz-Castro, F., et al., *Mifepristone for Treatment of Metabolic Syndrome: Beyond Cushing's Syndrome.* Front Pharmacol, 2020. **11**: p. 429.
5. Feelders, R.A., et al., *Advances in the medical treatment of Cushing's syndrome.* Lancet Diabetes Endocrinol, 2019. **7**(4): p. 300-312.
6. Jones, T.K., et al., *Discovery of novel intracellular receptor modulating drugs.* J Steroid Biochem Mol Biol, 1996. **56**(1-6 Spec No): p. 61-6.
7. Cuevas-Ramos, D., D.S.T. Lim, and M. Fleseriu, *Update on medical treatment for Cushing's disease.* Clin Diabetes Endocrinol, 2016. **2**: p. 16.
8. Hunt, H.J., et al., *Identification of the Clinical Candidate (R)-(1-(4-Fluorophenyl)-6-((1-methyl-1H-pyrazol-4-yl)sulfonyl)-4,4a,5,6,7,8-hexah ydro-1H-pyrazolo[3,4-g]isoquinolin-4a-yl) (4-(trifluoromethyl)pyridin-2-yl)methano ne (CORT125134): A Selective Glucocorticoid Receptor (GR) Antagonist.* J Med Chem, 2017. **60**(8): p. 3405-3421.
9. Hunt, H., et al., *Assessment of Safety, Tolerability, Pharmacokinetics, and Pharmacological Effect of Orally Administered CORT125134: An Adaptive, Double-Blind, Randomized, Placebo-Controlled Phase 1 Clinical Study.* Clin Pharmacol Drug Dev, 2018. **7**(4): p. 408-421.
10. Spaanderman, D.C.E., et al., *Androgens modulate glucocorticoid receptor activity in adipose tissue and liver.* J Endocrinol, 2018.
11. Koorneef, L.L., et al., *The selective glucocorticoid receptor antagonist CORT125281 has tissue-specific activity.* J Endocrinol, 2020.
12. Rensen, P.C., et al., *Selective liver targeting of antivirals by recombinant chylomicrons--a new therapeutic approach to hepatitis B.* Nat Med, 1995. **1**(3): p. 221-5.
13. Kroon, J., et al., *Selective Glucocorticoid Receptor Antagonist CORT125281 Activates Brown Adipose Tissue and Alters Lipid Distribution in Male Mice.* Endocrinology, 2018. **159**(1): p. 535-546.
14. Gasparini, S.J., et al., *Androgens sensitise mice to glucocorticoid-induced insulin resistance and fat accumulation.* Diabetologia, 2019. **62**(8): p. 1463-1477.
15. Kaikaew, K., et al., *Sex Difference in Corticosterone-Induced Insulin Resistance in Mice.* Endocrinology, 2019. **160**(10): p. 2367-2387.
16. Kroon, J., A.M. Pereira, and O.C. Meijer, *Glucocorticoid Sexual Dimorphism in Metabolism: Dissecting the Role of Sex Hormones.* Trends Endocrinol Metab, 2020. **31**(5): p. 357-367.
17. Ruiz, D., V. Padmanabhan, and R.M. Sargis, *Stress, Sex, and Sugar: Glucocorticoids and Sex-Steroid Crosstalk in the Sex-Specific Misprogramming of Metabolism.* J Endocr Soc, 2020. **4**(8): p. bvaa087.
18. Kroon, J. and O.C. Meijer, *Sex and Stress Steroid Crosstalk Reviewed: Give Us More.* J Endocr Soc, 2020. **4**(10): p. bvaa113.
19. Santilli, F., et al., *Metabolic Syndrome: Sex-Related Cardiovascular Risk and Therapeutic Approach.* Curr Med Chem, 2017. **24**(24): p. 2602-2627.
20. Cuevas-Ramos, D. and M. Fleseriu, *Medical treatment of Cushing's Disease.* Minerva Endocrinol, 2016. **41**(3): p. 324-40.
21. Koorneef, L.L., et al., *Selective Glucocorticoid Receptor Modulation Prevents and Reverses Nonalcoholic Fatty Liver Disease in Male Mice.* Endocrinology, 2018. **159**(12): p. 3925-3936.

22. van den Heuvel, J.K., et al., *Identification of a selective glucocorticoid receptor modulator that prevents both diet-induced obesity and inflammation.* Br J Pharmacol, 2016. **173**(11): p. 1793-804.
23. Mylka, V., et al., *The autophagy receptor SQSTM1/p62 mediates anti-inflammatory actions of the selective NR3C1/glucocorticoid receptor modulator compound A (CpdA) in macrophages.* Autophagy, 2018. **14**(12): p. 2049-2064.
24. Nguyen, E.T., et al., *Effects of combined glucocorticoid/mineralocorticoid receptor modulation (CORT118335) on energy balance, adiposity, and lipid metabolism in male rats.* Am J Physiol Endocrinol Metab, 2019. **317**(2): p. E337-E349.
25. Shen, Y., et al., *Adipocyte glucocorticoid receptor is important in lipolysis and insulin resistance due to exogenous steroids, but not insulin resistance caused by high fat feeding.* Mol Metab, 2017. **6**(10): p. 1150-1160.
26. Sun, W., et al., *snRNA-seq reveals a subpopulation of adipocytes that regulates thermogenesis.* Nature, 2020. **587**(7832): p. 98-102.

ACKNOWLEDGEMENTS

The authors thank Trea Streefland and Amanda Pronk for their valuable technical assistance, and Sygnature Discovery for synthesizing novel glucocorticoid antagonists and early phase *in vitro* assessment of glucocorticoid receptor antagonists.

APPENDIX

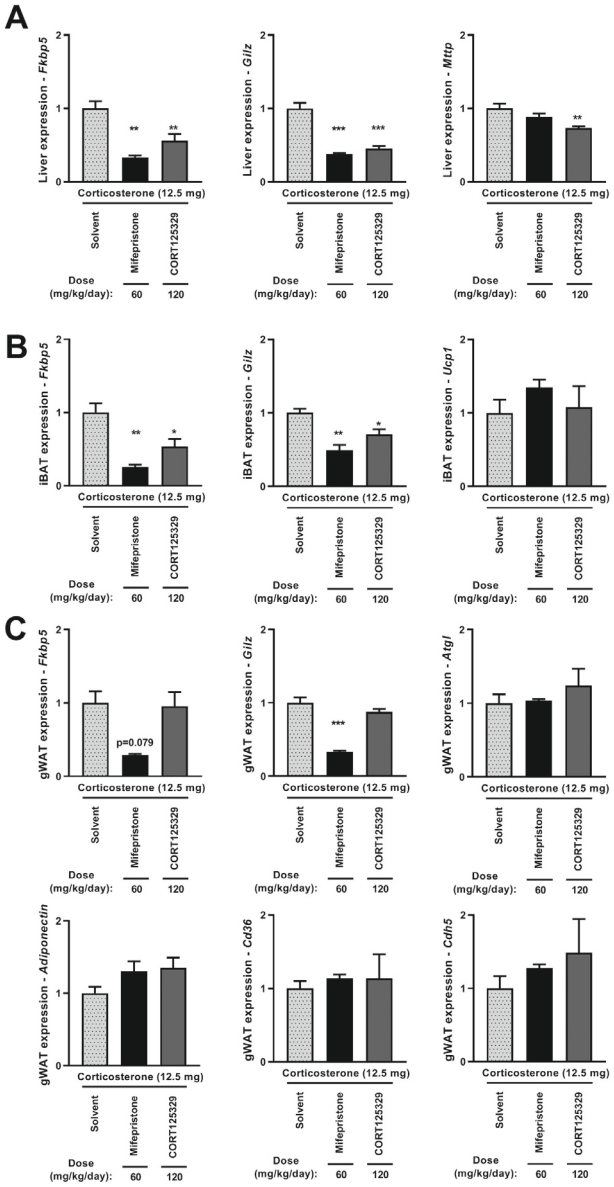

Supplementary Figure 1. GR antagonism by CORT125329 is tissue specific. RT-PCR analysis of **(A)** livers, **(B)** interscapular brown adipose tissue (iBAT) and **(C)** gonadal white adipose tissue (gWAT) obtained from male C57Bl/6J mice exposed to sub-chronic corticosterone and treatment with solvent, 60 mg/kg/day mifepristone or 120 mg/kg/day CORT125329. Statistical differences were calculated using a one-way ANOVA with Tukey's multiple comparisons test. *p<0.05 vs solvent, **p<0.01 vs solvent, ***p<0.001 vs solvent.

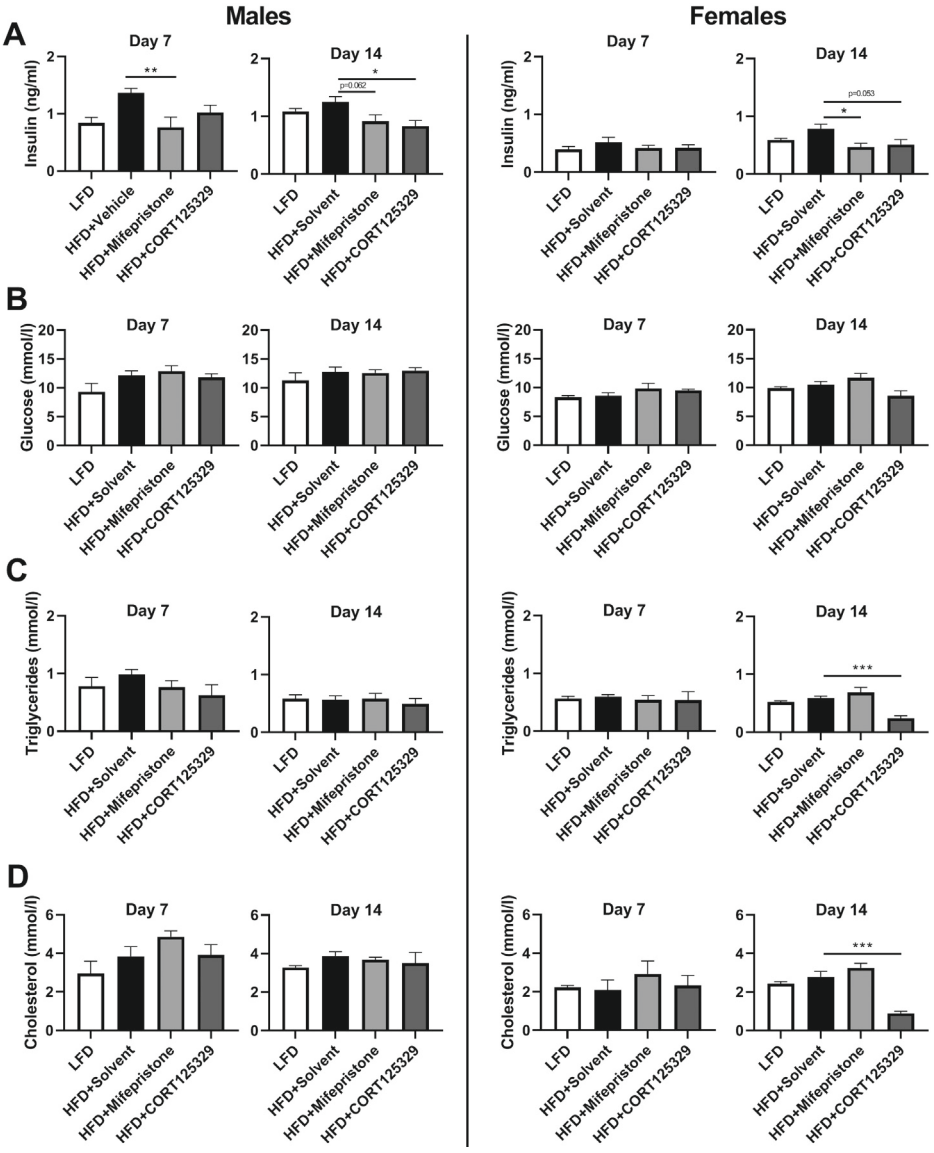

Supplementary Figure 2. The effect of mifepristone and CORT125329 on plasma biochemistry of male and female mice exposed to short-term high-fat diet. The effect of daily solvent, mifepristone or CORT125329 treatment on **(A)** plasma insulin, **(B)** glucose, **(C)** triglycerides and **(D)** cholesterol levels in male and female mice at day 7 and 14. Statistical differences were calculated using a one-way ANOVA with Dunnett's multiple comparisons test. *p<0.05, **p<0.01, ***p<0.001. Abbreviations: LFD = low-fat diet, HFD = high-fat diet.

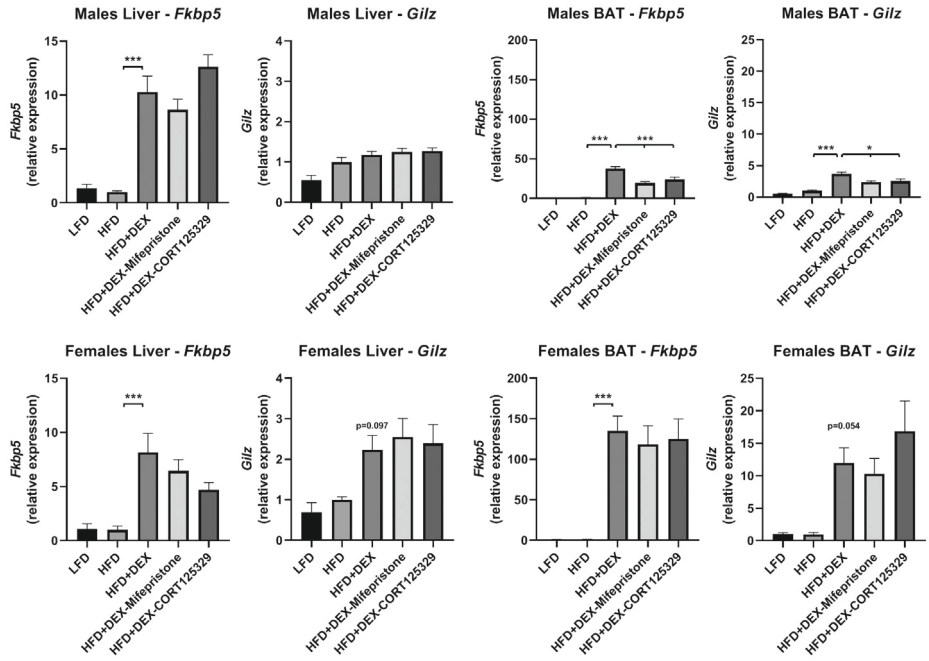

Supplementary Figure 3. The effect of mifepristone and CORT125329 on dexamethasone-induced GR activity in liver and brown adipose tissue. The effect of daily solvent, mifepristone or CORT125329 treatment on dexamethasone-induced expression of GR-responsive genes *Fkbp5* and *Gilz* in the liver and brown adipose tissue (BAT) of male and female mice exposed to short-term high-fat diet. Statistical differences were calculated using a one-way ANOVA with Dunnett's multiple comparisons test. *p<0.05, ***p<0.001.

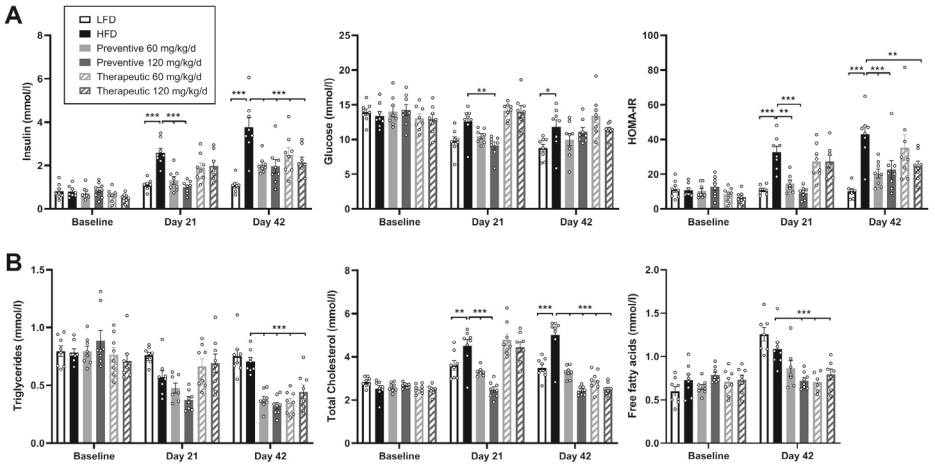

Supplementary Figure 4. The effect of CORT125329 on plasma biochemistry in male mice exposed to long-term high-fat diet. The effect of preventive or therapeutic treatment with 60 and 120 mg/kg/day CORT125329 on **(A)** plasma insulin and glucose, and the HOMA-IR index, and on **(B)** plasma triglycerides, cholesterol and free fatty acids. Statistical differences were calculated using 2-way ANOVA with Tukey's multiple comparisons test. *p<0.05, **p<0.01, ***p<0.001.

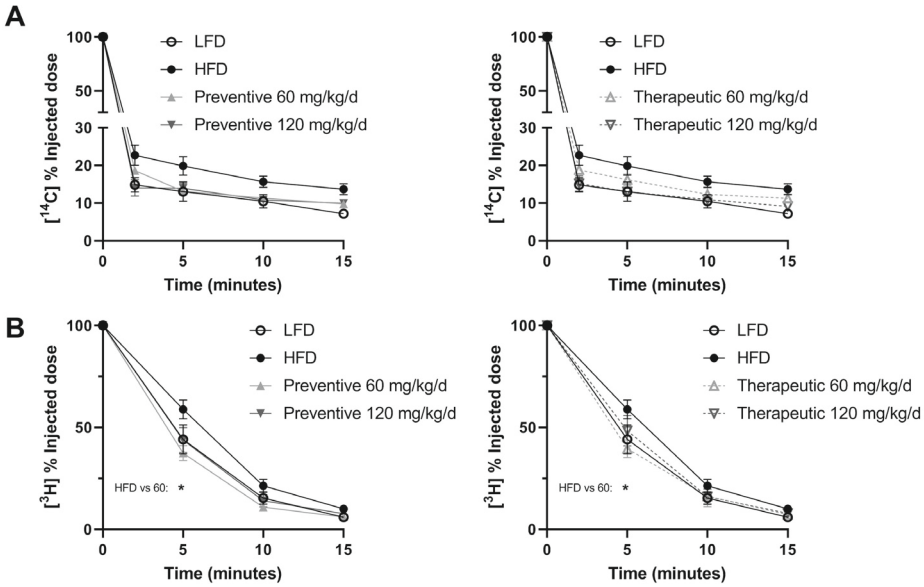

Supplementary Figure 5. The effect of CORT125329 on plasma clearance of [^{14}C] deoxyglucose and [^{3}H] oleate in male mice exposure to long-term high-fat diet. The effect of preventive or therapeutic treatment with 60 and 120 mg/kg/day CORT125329 on plasma decay of **(A)** [^{14}C] deoxyglucose and **(B)** [^{3}H] oleate. Statistical differences were calculated using a 2-way ANOVA with Dunnett's multiple comparisons test. *p<0.05.

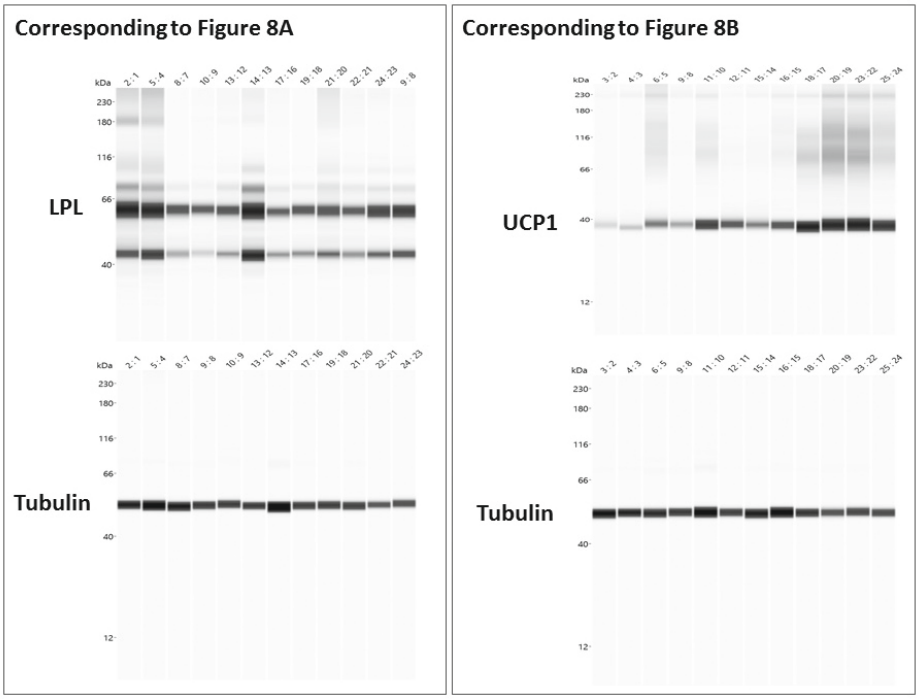

Supplementary Figure 6. The effect of CORT125329 on LPL and UCP1 protein expression. Uncropped western blot images of LPL, UCP1 and tubulin protein expression. Corresponds to Figure 8A-B.